



# Development of Mitsubishi "i" Body

Hayami NAKAGAWA\* Yoshinobu MATSUMURA\* Shigeru ITO\*  
 Akio SHIRATORI\* Masahiro YOSHIDA\*\* Koji FUJII\*\*  
 Hisao MORI\*\* Satoshi YANAGIMOTO\*\*\* Kazuhiro UESHIRO\*\*\*

## Abstract

Recently, the technology to develop a vehicle body with high strength, high rigidity and light weight has become increasingly necessary for the automotive industry to improve crashworthiness and reduce CO<sub>2</sub> emissions. This paper presents one of the solutions from Mitsubishi Motors Corporation (MMC) to meet the above demands. MMC developed a lightweight aluminum space-frame body with a view toward mass production at relatively low cost, and applied it on the Mitsubishi "i". In addition, the aerodynamic characteristics of the body shape were fine tuned for reduced driving resistance, which successfully achieved very low drag (C<sub>D</sub>).

*Key words:* Body, Aluminum, Space Frame, Weight Reduction, Aerodynamics, Life Cycle Assessment

## 1. Introduction

Improvements in crashworthiness and quietness, and installation of more interior equipment (for example, navigation and entertainment systems) have resulted in increasingly heavy passenger cars. However, growing demand for further reduced fuel consumption as a means of combating global warming, oil-resource depletion, and other environmental problems has created a critical need for automotive manufacturers to produce lighter vehicles.

An all-aluminum vehicle body is one means of achieving the necessary weight savings. Research and development on all-aluminum bodies have been conducted and some all-aluminum body models have already been marketed, but their application is thus far limited to a small number of production models mainly because of high material costs.

MMC developed and applied on the "i" an aluminum space-frame body that is highly strong and rigid but relatively inexpensive to produce, aiming primarily at achievement of ultra-low fuel consumption and with a view to mass-producing aluminum space-frame bodies in the future.

Recognizing improved aerodynamics as essential for realizing low fuel consumption, MMC also made exhaustive research and improvements for low C<sub>D</sub> value of the "i" body. An overview of this body is given in this paper.

## 2. Aluminum space-frame body

An all-aluminum body can be constructed using

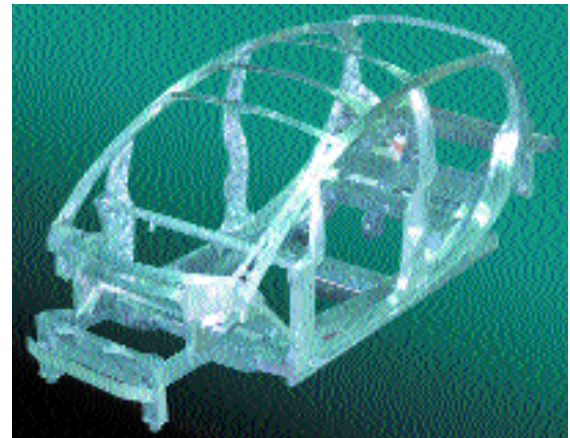


Fig. 1 Space-frame of "i"

either a space-frame structure or monocoque structure. For the "i", MMC opted for an aluminum body with space-frame construction (Fig. 1), which serves to keep production costs relatively low and hence is advantageous in view of future mass production. Mitsubishi Aluminum Co., Ltd. collaborated with MMC in developing the aluminum space-frame body.

The body's basic framework is formed from aluminum extrusions and aluminum die-castings, which are laid out and combined for optimal effectiveness. The floor and roof panels are formed from aluminum pressings.

The merits of extrusions include low die costs and a good yield factor, so detailed structural studies were performed to enable maximal use of extrusions

\* Advanced Vehicle Development Department, Research & Development Office

\*\* Studio Package Engineering Department, Research & Development Office

\*\*\* Body Production Engineering Department, Global Production Office

\*\*\* Environment & Technical Affairs Department, Group Corporate Strategy Office

\*\*\* Automotive Development Department, Mitsubishi Aluminum Co., Ltd.

\*\*\* Machinery & Environment Plant Department, Kobe Shipyard & Machinery Works, Mitsubishi Heavy Industries, Ltd.

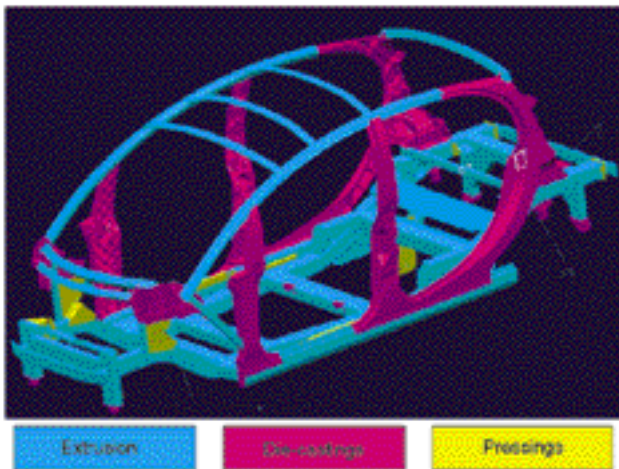


Fig. 2 Types of space-frame members



Fig. 3 Cross-sectional view of extrusion forming dash cross member lower

throughout the body. As a result, extrusions account for approximately 60 % of the weight of the body-in-white (Fig. 2).

## 2.1 Plastic working techniques for aluminum material

### (1) Extrusions

An extrusion is formed as a continuous closed-section member. The thickness of each wall constituting the cross section can be established as desired (Fig. 3). Compared with a monocoque structure, which consists of spot-welded pressings, a space-frame structure based mainly on extrusions allows high strength and rigidity to be achieved more efficiently. Many extrusions were applied for the "i" body including side members and cross members of the underbody and the roof side rails and roof bows of the upper body.

A6N01 was selected for the material from the 6000-series alloys that offer low cost and good extrudability, considering corrosion resistance and weldability. The tensile strength of the side members, side roof rails, and other bent members was increased by means of artificial ageing applied after the bending processes.

The side members (the main frame members of the underbody) are made of one-piece bending-formed aluminum extrusions, extending from the front of the vehicle to the rear (Fig. 4). This helps to minimize the number of parts and joints, thereby saving weight while helping to maximize rigidity. For the joints between the side members and cross members, a through-holes



Fig. 4 One-piece side member

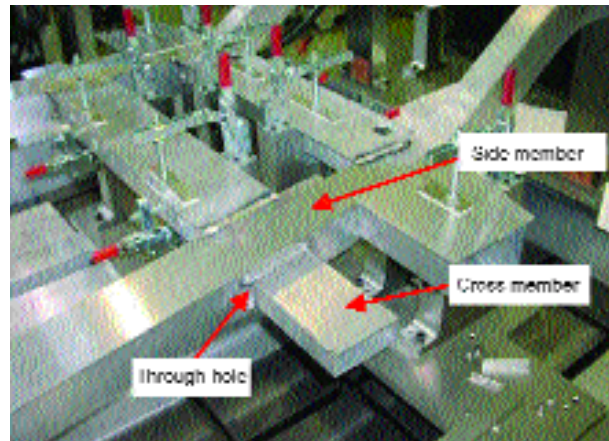


Fig. 5 Through-hole structure

structure (Fig. 5) was adopted, which eliminated nodes\*1. This joint structure reduces distortion of the welds and improves the strength of the joints.

\*1: Node refers to die-cast pieces used for joints between frame members.

### (2) Die-castings

Die-castings were applied for portions like the front pillars and center pillars because extrusions were not suitable for satisfying styling requirements as well as structural requirements including strength and trim-part retention. A specific advantage of die-castings is that they permit the consolidation of multiple parts (including those for attachment of trim parts) into single parts and thus enable minimization of material and tooling costs (Fig. 6).

The high-vacuum die-casting method was employed, by which the amount of gas mixing with the molten aluminum could be reduced and thus high welding stability was ensured. In addition, this method enabled the material thickness to be minimized for further lightness (Fig. 7).

### (3) Pressings

Pressings made of a 6000-series alloy (the same series as that used for extrusions) were adopted for the floor, dash panel, roof, and quarter panels (Fig. 8). Specifically, the material is MX699, which is produced by Mitsubishi Aluminum Co., Ltd. A coating of lubricant on MX699 yields improved press formability, so this material can be employed for parts that are relatively difficult to press-form.

## 2.2 Joining technology

### (1) Hybrid laser welding

Extrusions and die-castings are typically joined by



Fig. 6 Front pillar

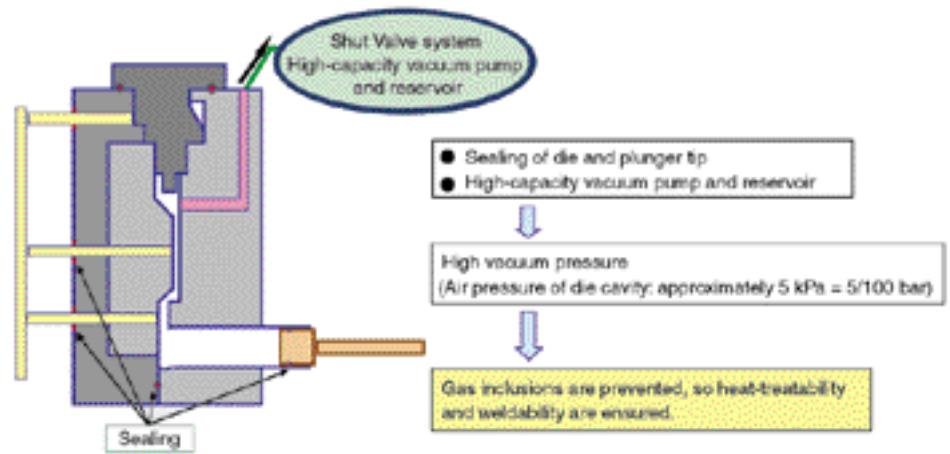


Fig. 7 Schematic diagram of high-vacuum die-casting molds

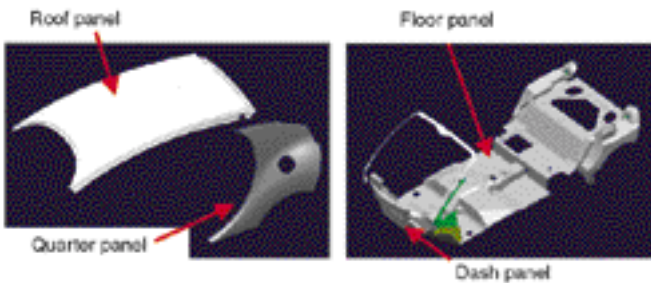


Fig. 8 Pressings

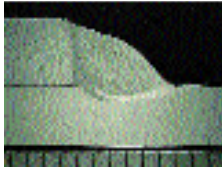
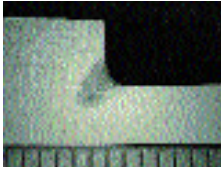
	MIG-YAG 4 kW + 280 A	YAG alone 4 kW
3 m/min t 4 mm AC4C + 5000 series		

Fig. 9 An example of welds on aluminum alloy


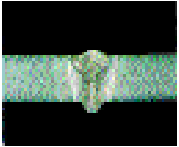

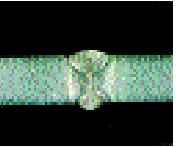



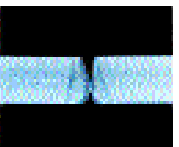
Gap (mm)	0	0.5	1.0	1.5
MIG-YAG 5 kW, 125 A, 18 V 0.8 m/min				
YAG alone 5 kW 0.8 m/min				

Fig. 10 Gap allowance

means of MIG welding or TIG welding. The "i" body, however, employed hybrid laser welding (a type of welding that combines laser welding and arc welding) in order to ensure superior joint strength and body dimensional precision. Among the MIG, TIG and plasma methods for arc welding, the MIG method was selected and combined with the YAG method that was selected as laser welding technique. MIG-YAG hybrid laser welding was selected because it is suitable for aluminum welding and allows gap tolerance.

MIG-YAG hybrid laser welding provides the MIG-based benefit of gap tolerance resulting from weld overlay, and provides the YAG-based benefit of deep penetration (Fig. 9). As a result, it gives consistent weld

strength even when slight gaps exist between welded parts. Fig. 10 illustrates the superior gap tolerance of MIG-YAG hybrid laser welding; with YAG laser welding alone, a gap of 1 mm or more causes the laser to pass through the material, resulting in a failed weld, but with the hybrid arrangement, stable welding is possible with a gap up to 1.5 mm. Furthermore, MIG-YAG hybrid laser welding can be performed approximately three times as quickly as MIG welding alone. Since heat input into the workpieces is smaller, welds are distorted relatively little and resulting body dimensions are highly precise. Fig. 11, Fig. 12, and Table 1 give an overview of the coaxial MIG-YAG hybrid laser head (made by Mitsubishi Heavy Industries, Ltd.) used for welding the

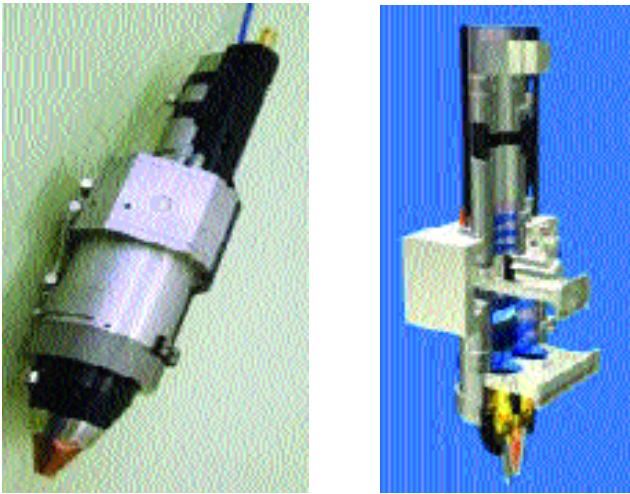


Fig. 11 Appearance and cut model of coaxial MIG-YAG hybrid laser head

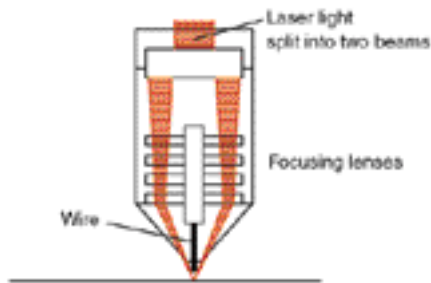


Fig. 12 Schematic of coaxial MIG-YAG hybrid laser head

"i" body. Inside the head, laser light is split into two beams by an optical mirror arrangement and the arc electrode and wire feed passage are positioned coaxially between the two laser beams. This structure realizes compact dimensions and permits good robot maneuverability (Fig. 13).

#### (2) Self-piercing rivets (SPRs)

SPRs, which are comparable with conventional spot welds in terms of shear strength and separation strength, were adopted for such lap joints as those between pressings and extrusions where relatively high joint strength is required. This method uses rivets that are coated to prevent electric corrosion for joining parts positioned on top of another by driving the rivets into the parts. In addition to offering high joint strength, this method also enables the joining of different materials (Fig. 14).

### 3. Plastic outer panels

Plastics that combine lightness with superior damage resistance were adopted for the body's outer panels.

In addition to the bumpers that usually have been made of plastics, the fenders, hood and tail gate were also made of plastics, which not only reduced the weight of these parts but also provided them with good restorability after low-speed collision.

A newly conceived plastic module construction was

Table 1 Specifications of coaxial MIG-YAG hybrid laser head

Item	Specification
Dimensions	400 x 100 x 100 mm
Weight	5 kg
Laser power	< 5 kW
Arc current	< 300 A
Focal length	145 mm
Focusing ratio	1 : 1
Optical fiber	0.6 mm

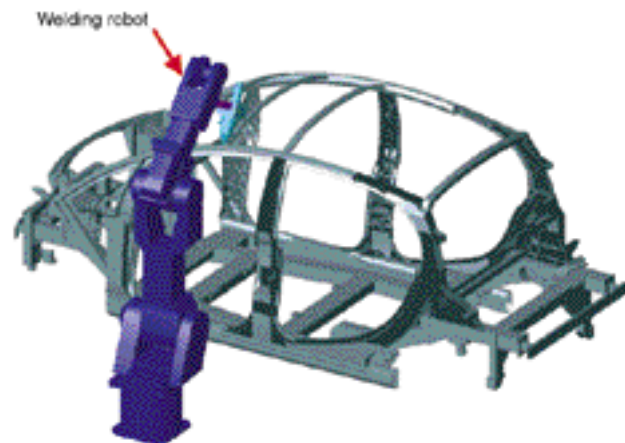


Fig. 13 Welding process simulation

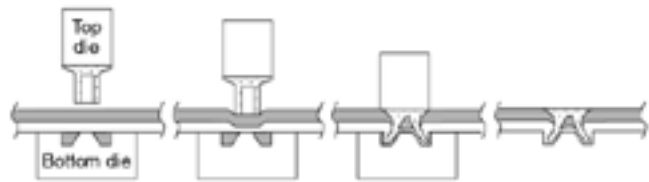


Fig. 14 SPR joining process

adopted for the doors. With each door, a plastic outer molding is fitted over a plastic inner molding that serves both as an interior trim part and as a structural member of the door. The window regulator, window motor, and other functional parts are mounted on the outer side of the inner molding.

A high-strength polycarbonate material was adopted for the door and tailgate windows. This material has a coating that resists scratching and helps to prevent fogging.

## 4. Basic properties of body framework

### 4.1 Rigidity, strength, and weight

The cross-sectional profile of the extrusions was designed to realize static flexural and static torsional rigidity comparable with that of a steel monocoque body (Fig. 15).

Since the underbody was, as stated, constructed using extrusions (each of which has a continuous cross section) and thus has a significantly higher level of rigidity than that of a steel monocoque structure, it facilitated further weight savings in the upper body.

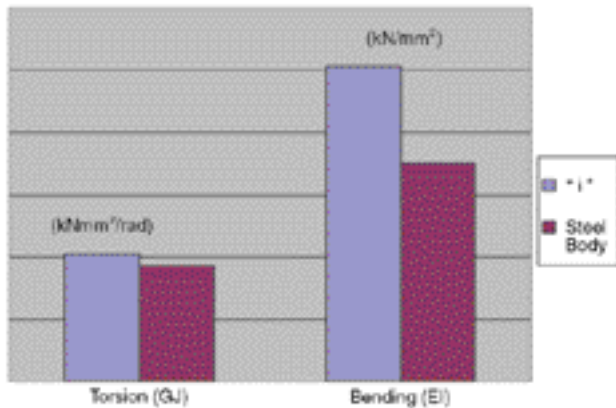


Fig. 15 Static rigidity: "i" body vs. steel body

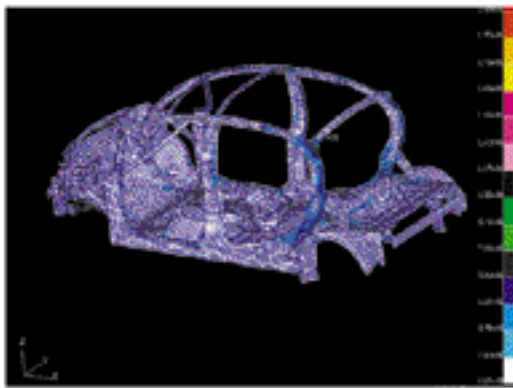


Fig. 16 CAE analysis of static rigidity

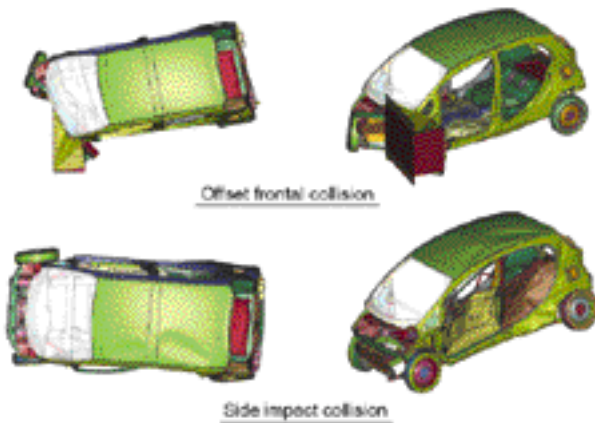


Fig. 17 CAE analysis of crashworthiness

Regarding the strength, joint structure and reinforcement layout throughout the body was decided with a view to minimizing the possibility of stress concentrations in welded areas (Fig. 16).

By adopting an aluminum space frame, it was possible to make the "i" body-in-white approximately 110 kg lighter than a steel monocoque body with the same levels of strength and rigidity.

#### 4.2 Crashworthiness

One of the most significant attributes of the "i" is that it offers high crashworthiness and pedestrian-protection performance despite its compact body dimen-

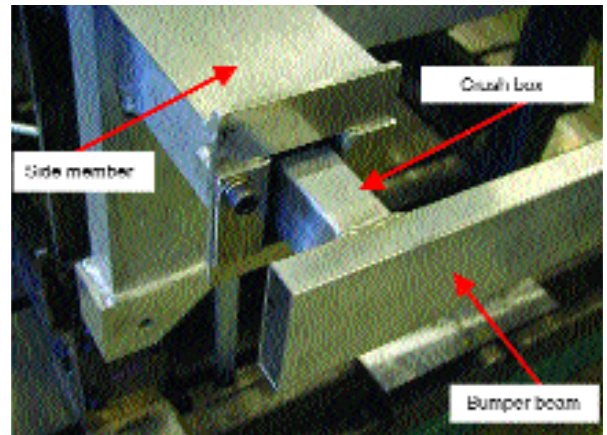


Fig. 18 Crush box

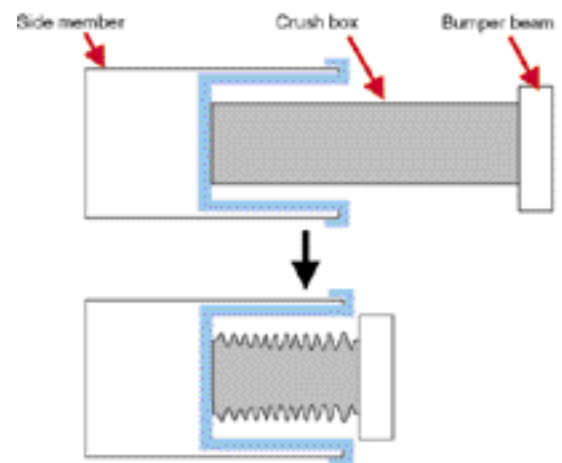


Fig. 19 Image of crush box behavior in crash

sions. Indeed, the "i" leads its class by meeting the requirements for the European New Car Assessment Programme ratings of four stars for crashworthiness and three stars for pedestrian protection (Fig. 17).

The "i" has a midship engine, so it was possible to achieve a long crush length at the front of the body and significant energy absorption in the hood. Energy absorption in a frontal collision and protection for pedestrians are both greatly enhanced.

Optimized cross-sectional profile in the straight, extruded side members and beads that can buckle at the front end of each side member yield ideal compression-load characteristics in the event of a crash, ensuring that collision energy is efficiently absorbed. The amount of collision energy reaching cabin occupants is thus minimized.

Furthermore, crush boxes that take advantage of the properties of aluminum extrusions were adopted to minimize damage to the body in the event of a low-speed, low-intensity collision (Fig. 18). A crush box is fitted inside each side member, and adequate crush length is provided for effectively attenuating shocks as it can accommodate a crushed box without causing it to protrude from the front end of the side member (Fig. 19). This arrangement helps to permit a short overhang both at the front and rear, which is one of the main

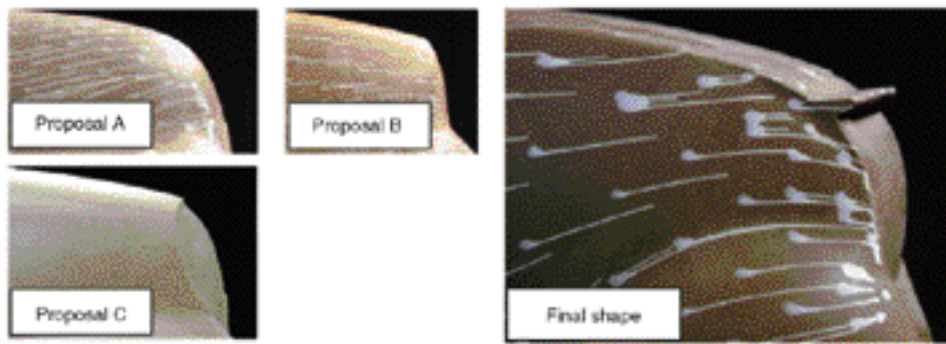


Fig. 20 Study of roof rear-edge shape using 1/4-scale model

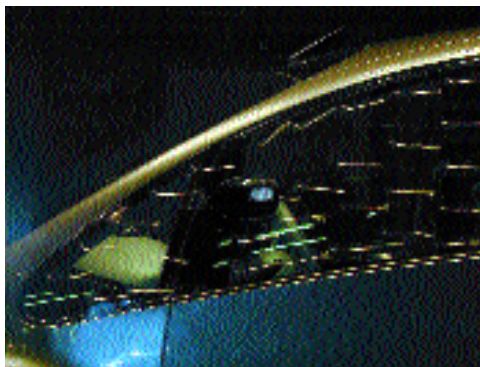


Fig. 21 Visualization of airflow around A-pillar



Fig. 22 Visualization of airflow around side mirror

styling and packaging features of the "i".

#### 4.3 Aerodynamic performance

Measures to minimize aerodynamic drag are vital for fuel economy. Indeed, aerodynamic drag at high speeds causes most of a vehicle's running resistance.

In the development of the "i", a 1/4-scale model and a full-size model were used in more than 500 wind-tunnel tests, and the results enabled an exceptionally low  $C_D$  of 0.24 to be achieved. Although the body reflects comprehensive measures to minimize aerodynamic drag, it also has attractive styling and permits efficient packaging. The combination of superior aerodynamic efficiency, styling, and packaging is one of the most significant attributes of the "i".

##### (1) Styling and aerodynamic performance

To give the body the required functionality while remaining faithful to the intentions of the stylists, who envisaged a body shape with entirely rounded contours, the aerodynamicists worked closely with the stylists and performed numerous wind-tunnel tests in pursuit of the final body shape.

The success with which the functional and aesthetic requirements were simultaneously satisfied is exemplified by the rear edge of the roof. The distinctive rounded shape of the roof initially inhibited smooth and consistent airflow separation at the rear edge and thus compromised the vehicle's drag coefficient and rear lift coefficient. Numerous wind-tunnel tests conducted on various rear-edge shapes (Fig. 20) led to the best possible solution.

Furthermore, although the rear spoiler is relatively small it is positioned at the optimal height, meaning that it yields a reduction of more than 10% in the vehicle's overall aerodynamic drag.

Significant effort was devoted also to the A-pillar contour between the windshield and each side window and to the shape of each side mirror. Consequently, vortices of the type formed near the A-pillars of a conventional vehicle by air flowing over the side windows are almost entirely prevented (Fig. 21) and the separation zone downstream of each door mirror is extremely small (Fig. 22).

##### (2) Packaging and aerodynamic performance

The "i" has a relatively short length and tall height, and it has short front and rear overhangs because its wheelbase is long relative to the overall length. These proportions are inherently disadvantageous for aerodynamic efficiency.

Although numerous wind-tunnel tests were conducted for optimization of the body shape, a great deal of additional effort was devoted to optimization of the front and rear fenders. Consequently, the flow field around each fender is almost entirely free of flow separation (Figs. 23 and 24).

A widely recognized means of achieving a low  $C_D$  value is to slant the roof downward at the rear edge. The roof of the "i" is smoothly curved downward toward the rear for this purpose, but it does not prevent the cabin from providing ample space for four adults. Exterior aerodynamic efficiency and interior practicality are thus both realized.



Fig. 23 Visualization of airflow around front fender



Fig. 24 Visualization of airflow around rear fender



Fig. 25 Undercovers

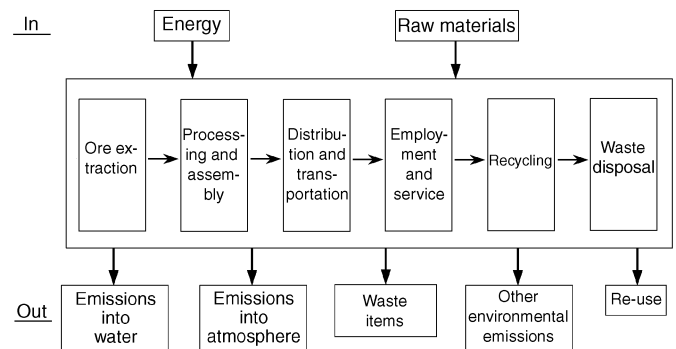


Fig. 26 Inventory analysis for lifecycle assessment

### (3) Underfloor airflow

Most of the body's bottom surface is provided with undercovers (Fig. 25) that form an ideally smooth surface for consistent airflow along with a low  $C_D$  value. The undercover's  $C_D$ -reducing effect is greater than 20% of the total drag reduction amount achieved in the "i".

Furthermore, air dams were adopted to control the airflow that is drawn into the wheel houses, thus suppressing the  $C_D$  value and helping to optimize the front/rear lift balance.

### (4) Cooling system

With the engine's cooling system, cooling air that has passed through the front of the body is fed through the condenser and radiator via ducts. Some of the air is then expelled into the wheel houses. The rest is fed through the clearance between the main floor and undercover to lower the temperature in the engine compartment and is expelled through an opening in the rear bumper. This arrangement raises the back pressure, i.e., reduces the vacuum pressure, at the rear surface of the body and thus helps to minimize aerodynamic drag.

## 5. Life Cycle Assessment (LCA)

The environmental impact ( $CO_2$  emissions) created by the aluminum materials and production technologies used for the "i" body were assessed.

An inventory analysis for the lifecycle was performed as shown in Fig. 26, and the amount of  $CO_2$

emissions was thereby verified. The object of comparison was a conventional steel body. A simulation was performed to investigate the extent to which the aluminum space-frame body of the "i" reduced  $CO_2$  emissions.

From the pre-extraction stage through the body-production stage, the amount of  $CO_2$  emissions for the "i" body was found to be greater than that for a steel body. Virgin (non-recycled) material was used for the aluminum pressings and extrusions; therefore, the larger amount of  $CO_2$  emissions was caused by electric smelting and other processes performed in production of the aluminum raw material.

At the usage stage, however, the "i" body's lightness (approximately 110 kg lighter than a steel body) contributes to superior fuel economy. As the distance driven increased, the higher  $CO_2$  emissions that occurred at the production stage were gradually offset. After approximately 20,000 km, the "i" body became superior to the all-steel body in terms of  $CO_2$  emissions (Fig. 27). This finding proves that the "i" body can provide a real advantage over the total-service-life distances driven in any country.

Next, case studies were performed for two assumed cases of future advances in recycling infrastructure (Table 2). With Case ①, the higher  $CO_2$  emissions caused during production were offset after approximately 13,000 km. With Case ②, where a higher rate of recyclability was assumed, the higher  $CO_2$  emissions caused during production were offset after approxi-

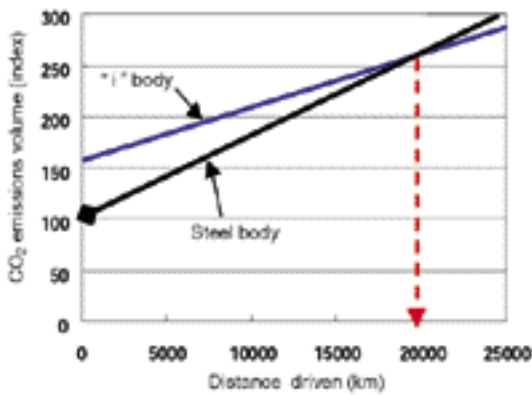


Fig. 27 Lifecycle CO<sub>2</sub> emissions comparison (case study)

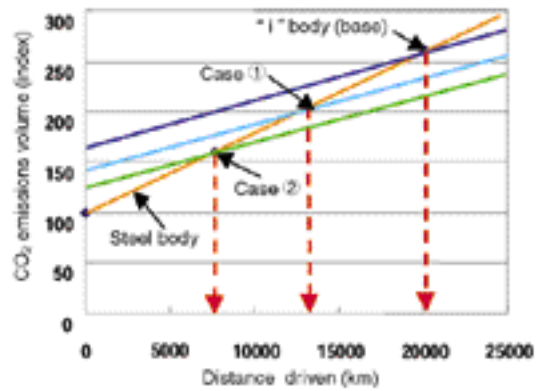


Fig. 28 Lifecycle CO<sub>2</sub> emissions comparison

Table 2 Aluminum recycling case study

	Rate of recyclability (%)		
	Die-castings	Pressings	Extrusions
Base	90	0	0
Case ①	90	50	50
Case ②	90	90	90

mately 8,000 km. Beyond these points, the relative lightness of the "i" body made it superior to the all-steel body in terms of total CO<sub>2</sub> emissions (Fig. 28).

As advances in recycling infrastructure are achieved, it will likely be possible to use recycled aluminum, meaning that the increase in CO<sub>2</sub> emissions at the production stage will be suppressed and that CO<sub>2</sub> emissions over the entire lifecycle will be further reduced.

It was also verified that the hybrid laser welding employed with the "i" body has no significant influence on the environmental burden created during body assembly.

The benefits of the aluminum body of the "i" with respect to lifecycle CO<sub>2</sub> emissions were thus confirmed. The potential for further reductions in lifecycle CO<sub>2</sub> emissions by means of improved material selection was also confirmed.

## 6. Conclusions

Significant weight savings in the body-in-white were realized by effective use of aluminum construction through the "i" project. In the near future, the demand for lighter bodies is expected to intensify as the need to save energy becomes more acute, and aluminum space-frame bodies are a means of meeting this demand. This project provided MMC with technologies and know-how for mass production of such bodies at relatively low cost. MMC will now work on ways to rationalize the aluminum space-frame structure so that

it is even easier to produce and even more commercially viable.

## 7. Acknowledgment

In developing the "i", high targets could be achieved thanks to extensive assistance from materials and production specialists. MMC wishes to express particular appreciation to the staff of the Automotive Development Department of Mitsubishi Aluminum Co., Ltd., who assisted with development tasks ranging from basic testing to CAE analysis and actual construction of "i".



Hayami NAKAGAWA



Yoshinobu MATSUMURA



Shigeru ITO



Akio SHIRATORI



Masahiro YOSHIDA



Koji FUJII



Hisao MORI



Satoshi YANAGIMOTO



Kazuhiro UESHIRO